

HARMONICS IN MVDC CABLE SYSTEMS – STUDY ON THERMAL AND ELECTRIC STRESS

Patrik Ratheiser^{1}, Shahtaj Shahtaj², Uwe Schichler¹, Brian G. Stewart²*

¹*Institute of High Voltage Engineering and System Performance, Graz University of Technology,
8010 Graz, Austria*

²*Institute for Energy and Environment, University of Strathclyde, G11XQ Glasgow, United Kingdom
patrik.ratheiser@tugraz.at

Keywords: MVDC CABLE, HARMONICS, MULTIPHYSICS SIMULATION, FIELD ENHANCEMENT

Abstract

MVDC can assist in resolving issues with the transition to renewable energy by expanding transmission capacity. Due to the use of converters, MVDC systems may be affected by harmonic currents and voltages. However, harmonics are not currently considered harmful in MVDC systems. Nevertheless, harmonics may have an impact on the electric field distribution and temperature in cable systems. Therefore, multiphysics FEM simulations are carried out to examine the general impact of harmonics in MVDC cables. The MVDC cable system experiences an electric field enhancement because of the influence of harmonics. The field enhancement shows the highest impact closest to the conductor. Furthermore, the average relative field enhancement is equal to the relative amplitudes of the harmonics. To investigate the field enhancement for different insulation material properties, different types of XLPE material (AC and DC) are investigated. Findings show that the influence of harmonic voltages rises with the non-linear conductivity of the insulation material. To examine the impact of harmonic currents on the ampacity of MVDC cable systems, FEM simulations are presented. The dielectric losses of MVDC cables compared to conductor losses are smaller than 0.01% and therefore negligible. Harmonic currents cause a very slight reduction in ampacity.

1 Introduction

The use of renewable energy sources has increased significantly to prevent future growth of carbon footprints. Consequently, long distance transmission and distribution lines are required, as most eco-friendly power plants are located far from consumer centres. In this regard, medium voltage (MV) direct current (DC) systems are becoming ever more important [1, 2]. Since MVDC is more effective for transmitting and distributing power over long distances than MV alternating current (AC), a better understanding of MVDC system operating conditions is necessary [3].

Nowadays, there is a growing interest in using MVAC equipment in DC operation. For this reason, a qualification procedure was introduced for the use of new or existing MVAC cable systems under DC stress [4]. In addition, an MVDC test procedure based on IEC 62895 and CIGRE TB 852, which were developed for HVDC cable systems, was proposed [5, 6]. Despite this, a special standard for MVDC systems is necessary to evaluate the system, as AC and DC, for example do not have the same breakdown mechanisms [7, 8]. Furthermore, the electric conductivity of the insulation under DC stress shows a strong non-linear behaviour dependent on temperature and electric stress [9].

As an emerging field, MVDC systems have not yet been explored in depth. However, there are already pilot projects like the prominent MVDC project ANGLE DC in Wales, United Kingdom and the MVDC demonstration E.ON Project “Preparation of a Medium-Voltage DC Grid Demonstration Project” in Germany. When compared to current MVAC

systems, these projects show better distribution capacities [10, 11]. Although harmonics have not been extensively investigated yet, they are not considered harmful in DC systems. However, harmonics from power electronic converters as well as from other sources are present in DC systems and require investigation [12].

The severity of harmonics in the ALBAHA power network, for example, was analysed when the MVDC link was introduced to the distribution system [13]. Voltage distortions were measured at various voltage levels and compared to the SERA standard limits [14]. The results indicate that the total harmonic distortions on the AC voltage are within standard limits. However, no study is available about the impact of harmonics on the electric field or ampacity in MVDC cables.

This contribution aims to investigate the electric field and ampacity of MVDC cable systems by considering harmonics (see Fig. 1). Multiphysics finite element method (FEM) simulations are carried out to investigate the electric field enhancement (FE) in the cable insulation. Thereby, different types of XLPE (AC and DC) are considered for comparison. Furthermore, the ampacity of different MVDC cable configurations and cross-sections is examined.

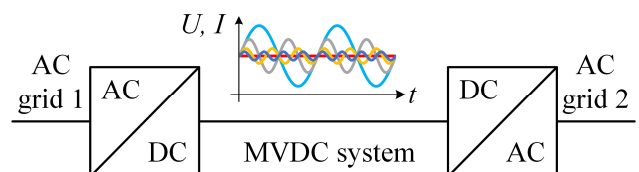


Fig. 1 Harmonics in MVDC cable system

2 Harmonics in DC Cable Systems

Since the early 1890s, transmission and distribution network voltage and current waveforms have been impacted by harmonic content [15]. Harmonics are important to consider in the power system because they have an impact on both the functionality of the equipment that utilises electricity and the quality of the electricity that is provided to consumers.

The schematic diagram of an exemplary DC link is shown in Fig. 2. At the sending end, an AC voltage output from any power source, such as wind, solar or conventional power plant is rectified to DC voltage (Point A). The DC voltage is inverted to an AC voltage at the receiving end (Point B), which matches the AC grid frequency. The power electronic converters enable AC/DC voltage conversion and vice versa [16].

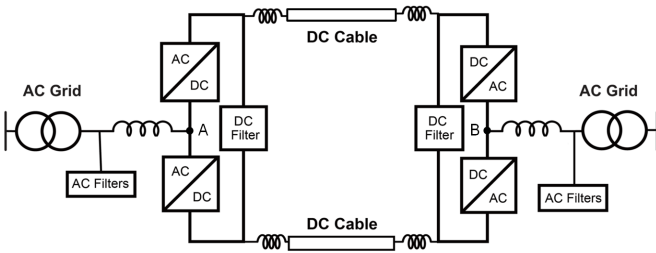


Fig. 2 Schematic diagram of an exemplary DC link [16]

Non-linear loads and power electronic converters are mainly responsible for generating harmonics in the DC power system. Loads depend on the consumer side, while the converters used in MVDC systems are mainly voltage source converters (VSC) (2-level, 3-level), which are executed, for example as modular multilevel converters (MMC) or neutral point-clamped (NPC) converters. The foundation of a modern MVDC system is comprised primarily of VSC [17]. However, MMC were employed in China's first multi-terminal MVDC project to show and provide dependable, high-quality power to the distribution networks [18]. Furthermore, the ANGLE DC project transforms 33 kV AC to ± 27 kV DC using a unique type of converter known as cascaded 3L-NPC VSCs with a switching frequency of 1 kHz [19, 20]. The converter's switching frequency determines the harmonic voltages' frequency content, which is a multiple of approx. six times the switching frequency (6 kHz) [20]. Therefore, an MVDC system's converter could cause disturbances that are superimposed on the DC output voltage, for example, harmonics on 6-pulse (Fig. 3(a)) and 12-pulse bridge converters (Fig. 3(b)) [21]. The resulting non-sinusoidal interference could be categorised as AC harmonic voltages.

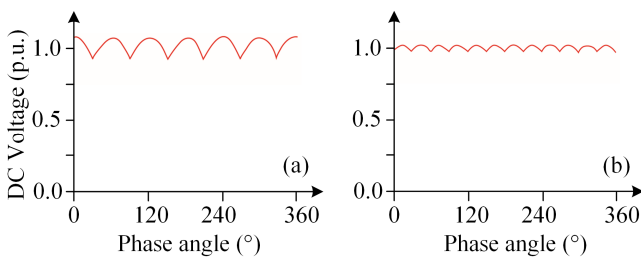


Fig. 3 Voltage over phase angle by using a (a) six-pulse and (b) twelve-pulse converter

A few studies have explored the development of various insulation degradation mechanisms such as partial discharges, water and electrical treeing which are influenced by harmonic distortions in DC cables [22]. Furthermore, electrical tree initiation and growth under DC superimposed AC have been studied, which demonstrates that an AC ripple can also be responsible for tree growth in insulation [23]. However, literature on how harmonic distortion affects the long-term performance and useful life of DC cables is scarce.

The lifetime of HVDC cable insulation and the insulation in cable accessories will be shortened by the combination of a DC voltage and an AC harmonic voltage, which will strain the insulation [16]. Nevertheless, for reliable operation and a knowledge of the effects of potential insulation degradation within the system, it is crucial to investigate the electric and thermal stress on DC cables due to harmonics.

3 Methodology

To investigate the impact of harmonic voltages on the electric field distribution in MVAC cables used for MVDC, multiphysics FEM simulations are carried out. The software "COMSOL" and the *Net-programmes from Mentor are used. Some of the results described in the paper were compared, and the deviation was smaller than 1%. The cable dimensions used in the multiphysics simulations are taken from the datasheet of a NA2XS(F)2Y 12/20 kV XLPE single core cable.

The thermal-electric simulations are performed with a defined temperature gradient across the insulation. The temperatures of the conductor (ϑ_c) and sheath (ϑ_s) were assumed to be fixed. The accumulation of space charges is not considered during the thermal-electric simulations.

To figure out the impact of harmonic voltages in relation to non-linear conductivity, three types of XLPE are investigated. One type is an AC-XLPE material and two types are DC-XLPE materials. Eq. (1) shows the parameters of the investigated AC-XLPE (σ_{AC}), while Eq. (2) and Eq. (3) describe the parameters of the investigated DC-XLPE. DC-XLPE 1 (σ_{DC1}) has a smaller temperature dependency in comparison to the AC-XLPE. DC-XLPE 2 (σ_{DC2}) shows a lower electric conductivity but a similar non-linear temperature dependency in comparison to the investigated AC-XLPE. However, DC-XLPE 2 has a smaller non-linear dependency on the electric stress. The apparent non-linear DC conductivity of the XLPE was determined during long-term measurements applying DC voltage without harmonics [24 – 26].

$$\sigma_{AC}(E, \vartheta) = 0.0425 \cdot e^{-\frac{0.872}{k_B \cdot \vartheta}} \cdot e^{\frac{0.541}{\vartheta} \cdot \sqrt{E}} \quad (1)$$

$$\sigma_{DC1}(E, \vartheta) = 10^{-29.12} \cdot e^{0.01 \cdot \vartheta} \cdot E^{1.95} \quad (2)$$

$$\sigma_{DC2}(E, \vartheta) = 3.28 \cdot E^{-1} \cdot e^{-\frac{0.56 \cdot q}{\vartheta \cdot k_B}} \cdot \sinh(2.77 \cdot 10^{-7} \cdot E) \quad (3)$$

In (1)–(3) σ is the electric conductivity in S/m, k_B the Boltzmann constant in eV/K, ϑ the temperature in K, E the electric stress in V/m, and q the elementary charge in C.

To simulate the electric stress from DC voltage combined with harmonics, firstly, current flow simulations are carried out to determine the electric field distribution under DC stress. Secondly, the electric field distribution caused by harmonics is simulated using time harmonic solutions. To determine the combined electric field stress, the superposition principle is used. The electric field distribution might show slight deviations in reality because the electric conductivity was not determined by applying DC voltage with harmonics.

To investigate the impact of harmonic currents on the ampacity of MVDC cable systems, thermal-magnetic simulations are performed. Fig. 4 shows the investigated models. They represent a bipolar cable system with two (M1) and six cables (M2). The simulations are performed for conductor cross-sections of $A = 240 \text{ mm}^2$ and $A = 1000 \text{ mm}^2$. The cables are presumed buried 1 m beneath the ground. The separation between the cables of model M2 is chosen with $d = 15 \text{ mm}$.

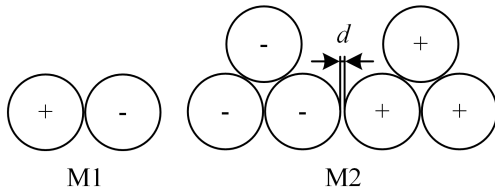


Fig. 4 Investigated MVDC cable models in thermal-magnetic FEM simulations

The most important material parameters for the FEM simulations are listed in Table 1. The remaining parameters are listed in [4, 27]. The cable conductor is aluminium, the shield copper and the sheath polyethylene. The cable insulation is made out of XLPE. The soil was simulated as "dry" within a radius of half a meter around the cable to account for soil drying in the FEM simulations. The remaining soil is considered "moist". The leakage current through the insulation was not considered in the cable heating calculations. This is permitted due to the negligible dielectric losses in MVDC cables, which are described in section 5.

Table 1 Material parameters used in multiphysics FEM simulations [27 – 30]

Material	Parameter	Value	Unit
XLPE	ϵ_r	2.3	1
	$\lambda_{20^\circ\text{C}}$	0.28	W/(m·K)
	c_p	2000	J/(kg·K)
	ρ_G	952	kg/m ³
	$\sigma(E, T)$	Eq. (1 – 3)	S/m
Soil	$\lambda_{20^\circ\text{C, moist}}$	1	W/(m·K)
	$\lambda_{20^\circ\text{C, dry}}$	0.4	W/(m·K)
	c_p	1200	J/(kg·K)
	ρ_G	1300	kg/m ³

Table 2 presents an overview of the simulations. The nominal DC voltage is chosen as $U_{\text{DC}} = \pm 55 \text{ kV}$. The amplitude and

frequency of the harmonic voltages correspond to the available data of a six-pulse converter [21]. The simulations are carried out for various conductor temperatures and temperature differences across the insulation.

Table 2 Overview of performed simulations

Simulation	Variables
DC + harmonic voltages with different conductor temperatures and temperature gradients	$\vartheta_i, \vartheta_o, \Delta\vartheta$ $\sigma(E, T)$
Transient thermal-magnetic simulations DC + harmonic currents	$Model, A, I$

4 Change of the Electric Field Distribution in MVDC Cables due to Harmonics

4.1 Electric field enhancement resulting from harmonics

The electric field distribution in MVDC cables at DC voltages combined with harmonics (U_{H}) is investigated. Table 3 shows harmonics produced for example by six-pulse converters, and considered in the thermal-electric FEM simulations [21].

Table 3 Harmonics produced by six-pulse converters

Harmonic order	Harmonic frequency	Relative amplitude $U_{\text{H}}/U_{\text{DC}}$	$U_{\text{H}} (U_{\text{DC}} = \pm 55 \text{ kV})$
6 th	300 Hz	0.0404	2222.0 V
12 th	600 Hz	0.0099	544.5 V
18 th	900 Hz	0.0044	242.0 V
24 th	1200 Hz	0.0025	137.5 V

Fig. 5 shows the results for $U_{\text{DC}} = \pm 55 \text{ kV}$ with (E_{H}) and without (E_{DC}) the harmonic voltages for the AC-XLPE. The conductor temperature is chosen with $\vartheta_{\text{C}} = 55^\circ\text{C}$. The cross-section of the cable is chosen with 240 mm^2 . The non-linear electric conductivity causes a field inversion for a temperature gradient of $\Delta\vartheta = 20 \text{ K}$. In addition, the impact of the harmonic voltages results in an FE in the DC cable system (Eq. (4)).

$$FE = \left(\frac{E_{\text{H}}}{E_{\text{DC}}} - 1 \right) \cdot 100\% \quad (4)$$

As shown in Fig. 5, FE rises near the conductor when a field inversion occurs. In this context, it is noteworthy that FE shows the highest values near the conductor ($r = 0 \text{ mm}$), where the electric stress is reduced due to the occurring field inversion resulting from the temperature gradient and the non-linear temperature dependency of the conductivity. FE lies between 4.9 – 6.8% without a temperature gradient and 4.0 – 8.6% with a temperature gradient of $\Delta\vartheta = 20 \text{ K}$ for the investigated AC insulation material. Furthermore, the impact of the harmonics on the electric field has an average value equal to the sum of the relative amplitudes of the occurring harmonics. This leads to an average FE of 5.72% when applying the harmonic voltages described in Table 3.

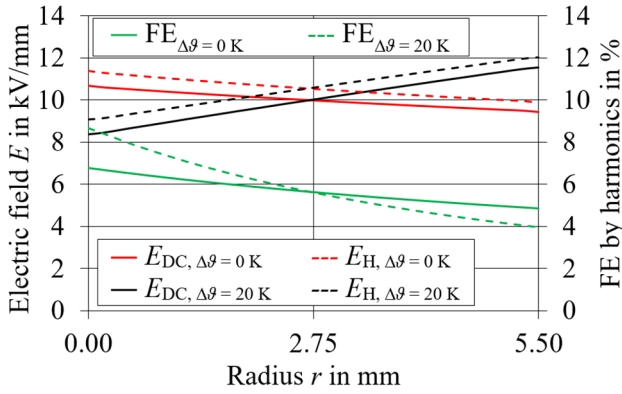


Fig. 5 Electric stress and FE with and without harmonics for $U_{DC} = \pm 55$ kV, $A = 240$ mm², a conductor temperature of $\vartheta_C = 55$ °C and at different temperature gradients

Fig. 6 shows the FE for $U_{DC} = \pm 55$ kV including the harmonic voltages listed in Table 3. The conductor temperature is set to $\vartheta_C = 90$ °C and the temperature gradient is varied. By comparison of FE in Fig. 5 and Fig. 6 ($\Delta\vartheta = 0$ K and 20 K) it can be seen that FE does not depend on the conductor temperature. However, it can be seen that FE increases with a higher temperature difference near the conductor and decreases near the shield, which relates to an even more pronounced field inversion. This is related to the electric field distribution according to the harmonics. The field distribution of harmonics shows the highest values near the conductor and the smallest near the shield. The FE for the investigated AC-XLPE is in between 3.9 – 8.9% for a temperature gradient up to $\Delta\vartheta = 25$ K.

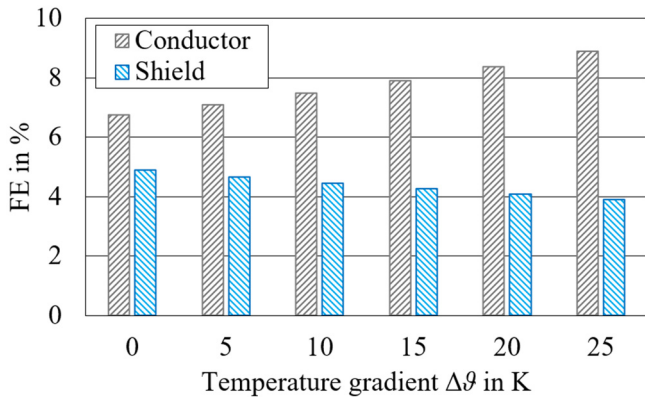


Fig. 6 FE for various temperature gradients at $\vartheta_C = 90$ °C for $U_{DC} = \pm 55$ kV and $A = 240$ mm²

4.2 Field enhancement caused by different XLPE materials

The electric field distribution in MVDC cables with different types of XLPE at DC voltages combined with harmonics (U_H) is investigated. These XLPE materials have a different behaviour in the DC conductivity. Fig. 7 shows the electric field distribution for a nominal DC voltage of $U_{DC} = \pm 55$ kV with harmonics and temperature differences of $\Delta\vartheta = 0$ K and 25 K for a conductor temperature of $\vartheta_C = 90$ °C. In comparison to the electric field distribution in AC-XLPE, the field inversion is not strongly pronounced for DC-XLPE 1. However, due to harmonics, FE lies between 4.7 – 7.0%. Nevertheless, in the

case of DC-XLPE 2, the harmonics result in an increase of FE between 4.0 – 8.6%, which is similar to the AC-XLPE. Therefore, the impact of harmonics rises with the non-linear conductivity and not with the value of the electric conductivity of the insulation material.

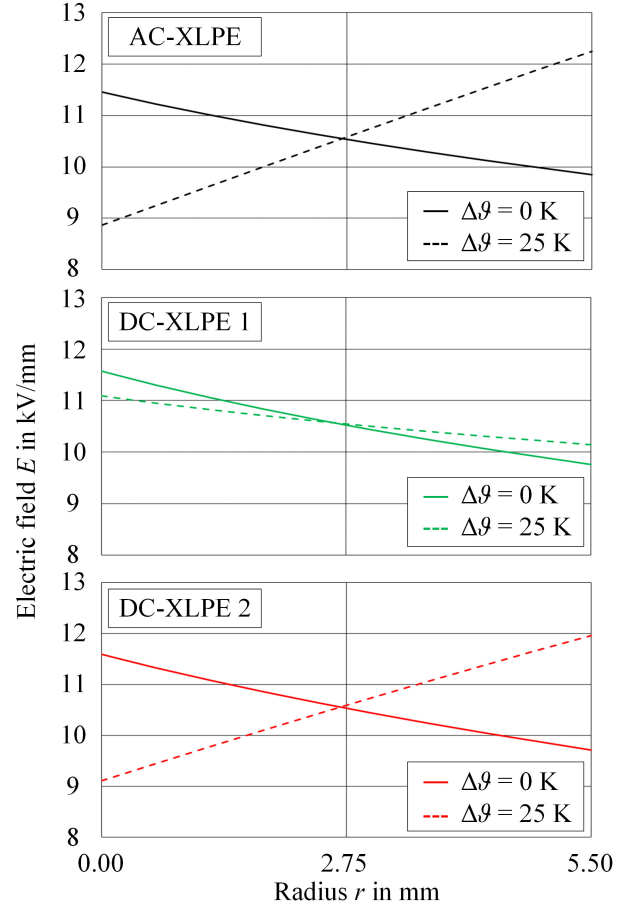


Fig. 7 Electric field distribution with harmonics from different XLPE materials used in MVDC cable systems

5 Ampacity in MVDC Cables considering Harmonics

To investigate the impact of harmonics on the ampacity of MVDC cables, FEM simulations are carried out. In reality, harmonic currents in DC systems strongly depend on the existing load. As no data is available for harmonic currents, the relative amplitudes are chosen according to the harmonic voltages in Table 3. This example demonstrates the impact of harmonic currents on the ampacity of a MVDC cable system. Table 4 shows the relative amplitudes of harmonic currents which are chosen to present the impact of harmonics on the ampacity. I_f is the content of harmonic currents for different frequencies. $I_{DC,H}$ is the ampacity considering harmonics.

Table 5 shows the simulation results of the two MVDC models for a conductor temperature of $\vartheta_C = 90$ °C. By including an overall 5.72% harmonic currents, the DC current $I_{DC,H}$ is reduced in comparison to the DC current without harmonics (I_{DC}) for both investigated models with different cross-sections by less than 0.2%. Therefore, the losses from the harmonics

seem to be negligible in this example. This is related to the losses in the conductor, which depend on $I^2 \cdot R(f)$, where $R(f)$ is the frequency dependent resistance of the conductor.

Table 4 Example harmonic currents in MVDC cables

Harmonic order	Harmonic frequency	Relative amplitude $I_f/I_{DC,H}$
6 th	300 Hz	0.0404
12 th	600 Hz	0.0099
18 th	900 Hz	0.0044
24 th	1200 Hz	0.0025

By calculating the ratio of the frequency dependent resistance ($R(f)$) and the DC resistance (R_{DC}) of the conductor, the ratio $R_{f=1200\text{ Hz}}/R_{DC}$ results in approximately 2 for a cross-section of $A = 240\text{ mm}^2$ and in approximately 6 for a cross-section of $A = 1000\text{ mm}^2$. The ratio decreases with lower frequencies of the harmonic currents. Due to this and the effective value of the harmonic currents, the total losses are nearly the sum of the individual losses from the occurring currents for the given example. When the sum of the conductor losses with and without harmonics reaches the same value, the same conductor temperature is reached, e.g. $\vartheta_C = 90\text{ }^\circ\text{C}$.

Table 5 Comparison of the ampacity of selected MVDC cable models with and without harmonics for $\vartheta_C = 90\text{ }^\circ\text{C}$

Model	M1		M2		
	A	240 mm ²	1000 mm ²	240 mm ²	1000 mm ²
I_{DC}		460.0 A	1028.0 A	438.0 A	687.0 A
$I_{DC,H}$		459.2 A	1025.3 A	437.0 A	685.5 A
$I_{f=300\text{ Hz}}$		18.6 A	58.6 A	25.0 A	27.7 A
$I_{f=600\text{ Hz}}$		4.5 A	14.4 A	6.1 A	6.8 A
$I_{f=900\text{ Hz}}$		2.0 A	6.4 A	2.7 A	3.0 A
$I_{f=1200\text{ Hz}}$		1.1 A	3.6 A	1.6 A	1.7 A

When investigating the temperature in MVDC cable systems according to harmonics, the dielectric losses have to be included in the consideration (Eq. 5).

$$P'_\delta = U_H^2 \cdot \omega \cdot C' \cdot \tan \delta \quad (5)$$

where P'_δ are the dielectric losses per meter, U_H is the harmonic voltage, ω is the angular frequency of the harmonic, C' is the capacitance per meter ($C' = 2.8 \cdot 10^{-10}\text{ F/m}$) and $\tan \delta$ is the loss factor ($\tan \delta = 2 \cdot 10^{-4}$).

The conductor losses to reach a conductor temperature of $\vartheta_C = 90\text{ }^\circ\text{C}$ are determined by using FEM simulations. For example, the conductor losses for model M2 ($A = 240\text{ mm}^2$) are $P_{C'} = 23.4\text{ W/m}$. The overall dielectric losses in comparison to the conductor losses in MVDC cables are $P'_\delta / P_{C'} = 2.65 \cdot 10^{-5}$ (Model M2). These losses are calculated from the occurring harmonic voltages at different frequencies with a frequency independent loss factor and capacitor of the

cable insulation. Due to the fact that the impact is less than 0.01%, these losses are negligible in MVDC systems.

6 Discussion

Nowadays, the proportion of acceptable harmonics in DC systems is agreed upon between the utilities and the manufacturers. However, this should be standardised in future because of their potential detrimental impact on the insulation material of cables. As described in section 4, the harmonic voltages in MVDC cables result in an FE. The FE depends on the amplitude of the harmonic voltages and the non-linear conductivity of the used insulation materials in this study. The FE may introduce partial discharges at the weakest points of the cable such as voids, and may lead to a breakdown in the insulation. The FE can be up to 9% by using the investigated XLPE materials. Also, higher values for FE might be reached when the insulation material has a stronger non-linear conductivity than the ones investigated. The FE results in a higher electric stress in the cable insulation, which can accelerate aging. The electric conductivity under a DC voltage with harmonics might also have a further impact on the electric field distribution. Additionally, the influence of space charge accumulation must be considered in future investigations.

By looking at the ampacity of MVDC cables, it can be seen that harmonic currents only increase the temperature to a small extent. Therefore, the considered harmonic currents do not have a strong impact on the ampacity. Nevertheless, the limits of harmonic currents will be of interest considering the heating. For academic completeness, the reduction of the current by applying twice of the harmonic currents mentioned in Table 4 was investigated. By taking $2 \cdot I_f/I_{DC,H}$, which results in an overall of 11.4% harmonics in the DC current, the ampacity has to be reduced by approximately 0.4% to keep the conductor temperature at $\vartheta_C = 90\text{ }^\circ\text{C}$. This is related to the dependency of the losses on $I^2 \cdot R(f)$. Due to the ratio of $R(f)/R_{DC}$ the losses depend mainly on the effective value of the currents for the mentioned frequencies and harmonic currents. The impact of the harmonic currents on the heating shows that harmonic currents are negligible in this example.

7 Conclusion

The behaviour of DC cables under various stresses is critical to ensure reliable operation. In addition to DC stress, DC cables are subjected to harmonics, which are produced by, e.g. power electronic converters. Harmonics in MVDC cables can cause, e.g. partial discharges in the cable system. Therefore, this contribution presents a methodology to investigate MVDC cables influenced by harmonic voltages and currents.

The thermal-electric simulations show that the electric field increases with a rise in harmonic voltages. Harmonics have the greatest influence on the electric field near the conductor. Furthermore, findings provide evidence that the FE caused by harmonics increases with the non-linear temperature dependency of the insulation material. To evaluate results in future studies more precisely, the electric conductivity

resulting from applying DC voltages with harmonics should be determined and space charges considered.

The influence of harmonic currents was investigated using thermal-magnetic simulations. It is shown that the thermal impact of dielectric losses according to harmonic voltages are negligible for MVDC cable systems. Furthermore, harmonic currents only show a small impact on the ampacity of MVDC systems. Given a sum of approximately 5.7% harmonic currents, the ampacity of a DC cable is reduced by less than 0.2% to reach an equal conductor temperature of $\vartheta_C = 90^\circ\text{C}$ in the MVDC cable system.

8 References

- [1] A. Williams and M. Thomson: 'Net Zero UK – Generation and Energy Storage Requirements for the UK to Become Carbon Neutral', *Journal of Energy and Power Technology*, Vol. 4(4), 2022.
- [2] A.J. Davis, N.S. Lewis, M. Shaner et al.: 'Net-zero emissions energy systems', *Science*, Vol. 360(6396), 2018.
- [3] G. Bathurst, G. Hwang and L. Tejwani: 'MVDC – The New Technology for Distribution Networks', 11th International Conference on AC and DC Power Transmission, Birmingham, United Kingdom, 2015.
- [4] P. Ratheiser and U. Schichler: 'Qualification of MVAC XLPE cables for DC operation', 22nd Int. Symposium on High Voltage Engineering (ISH 2021), Hybrid Conference, Report 118, Xi'an, China, pp. 179 – 184, 2021.
- [5] IEC 62895: 'High Voltage Direct Current (HVDC) Power Transmission – Cables with extruded Insulation and their Accessories for rated Voltages up to 320 kV for Land Applications – Test Methods and Requirements', 2017.
- [6] CIGRE WG B1.62: 'Recommendations for testing DC extruded cable systems for power transmission at a rated voltage up to and including 800 kV', CIGRE TB 852, 2021.
- [7] A. Buchner and U. Schichler: 'Review of CIGRE TB 496 regarding Prequalification Test on Extruded MVDC Cables', NORD-IS 19, Report 26, Tampere, Finland, 2019.
- [8] P. Ratheiser and U. Schichler: 'Review of IEC 62895 regarding Electrical Type Tests on extruded MVDC Cable Systems', Jicable HVDC'21, Report 16, Liège, Belgium, 2021.
- [9] P. Ratheiser and U. Schichler: 'MVAC XLPE Cables for MVDC – DC Conductivity of Plaque Samples During Temperature Changes', NORD-IS, Report 27, Trondheim, Norway, 2022.
- [10] J. Yu, K. Smith, M. Urizarbarrena et al.: 'Initial designs for the ANGLE DC project; converting existing AC cable and overhead line into DC operation', 13th Int. Conference on AC and DC Power Transmission, Manchester, United Kingdom, 2017.
- [11] F. Mura and R.W.D. Doncker: 'Preparation of a Medium-Voltage DC Grid Demonstration Project', E.ON Energy Research Center, Vol. 4(1), 2016.
- [12] W. Feng, L. Yang, F. Di et al.: 'Analysis of harmonic transmission characteristics in HVDC system', 2nd Conference on Energy Internet and Energy System Integration (EI2), Beijing, China, 2018.
- [13] T.A.H. Alghamdi and F.J. Anayi: 'Analysis of Harmonic Propagations in Albaha Power Network due to the Implementation of an MVDC Converter', IEEE PES Innovative Smart Grid Technologies - Asia (ISGT Asia), Brisbane, Australia, 2021.
- [14] Electricity and Cogeneration Regulatory Authority (ECRA): *Power Systems: Transmission and Distribution Code*, 2020.
- [15] A. Ganguli, A.K. Sharma and R. Ganguli: 'Harmonic Analysis in the Power System to Reduce Transmission losses and Save Energy', *Journal of Engineering Research and Applications*, Vol. 4(3), pp. 167 – 171, 2014.
- [16] A. Arshad and B.G. Stewart: 'Modelling Harmonic Propagation in HVDC System Power Cables', *Electrical Insulation Conference (EIC)*, Denver, USA, pp. 202 – 205, 2021.
- [17] G. Abeynayake, G. Li, T. Joseph et al.: 'Reliability Evaluation of Voltage Source Converters for MVDC Applications', *Innovative Smart Grid Technologies – Asia (ISGT Asia)*, Chengdu, China, pp. 2566 – 2570, 2019.
- [18] L. Qu, Z. Yu, Q. Song et al.: 'Planning and analysis of the demonstration project of the MVDC distribution network in Zhuhai', *Frontiers in Energy*, Vol. 13(1), pp. 120 – 130, 2019.
- [19] G. Abeynayake, J. Yu, A. Moon et al.: 'Analysis and Control of MVDC Demonstration Project in the UK: ANGLE-DC', *Power Supply*, Vol. 37(10), pp. 44 – 50, 2020.
- [20] A. Moon: 'Developments in the Angle-DC project: Project challenges, developments and findings to date', *Scottish Power Energy Networks*, 2018.
- [21] ALSTOM Grid: 'HVDC for Beginners and Beyond', ALSTOM Grid, 2010.
- [22] E. Corr, A. Reid, X. Hu et al.: 'Partial discharge testing of defects in dielectric insulation under DC and voltage ripple conditions', *CIGRE Sciences and Engineering*, pp. 117 – 125, 2018.
- [23] H. Zheng, G. Chen and S.M. Rowland: 'The influence of AC and DC voltages on electrical treeing in low density polyethylene', *International Journal of Electrical Power & Energy Systems*, Vol. 114(105386), 2020.
- [24] S. Qin and S. Boggs: 'Design considerations for high voltage DC components', *Electrical Insulation Magazine*, Vol. 28(6), pp. 36 – 44, 2012.
- [25] S. Hou, M. Fu, C. Li et al.: 'Electric field calculation and analysis of HVDC cable joints with nonlinear materials', 11th Int. Conference on the Properties and Applications of Dielectric Materials (ICPADM), Sydney, Australia, pp. 184 – 187, 2015.
- [26] P. Ratheiser and U. Schichler: 'DC Leakage Current Measurements: Contribution for the Qualification of extruded MVAC Cables for DC Operation', *Int. Conference on the Properties and Applications of Dielectric Materials (ICPADM)*, online, pp. 450 – 453, 2021.
- [27] P. Ratheiser, A. Buchner and U. Schichler: 'Übertragungskapazität von MGÜ-Kabelstrecken bei Verwendung von extrudierten AC-Mittelspannungskabeln', *VDE Hochspannungstechnik 2020*, pp. 371 – 376, online, 2020.
- [28] R. Bodega: 'Space Charge Accumulation in Polymeric High Voltage DC Cable Systems', PhD thesis, Delft University of Technology, 2006.
- [29] IEC 60287-3-1: 'Electric cables – Calculation of the current rating – Part 3-1: Operating conditions – Site reference conditions', 2014.
- [30] R. Woschitz, G. Komar, A. Pirker et al.: 'FEM-Simulation des thermischen Langzeit-Verhaltens von Hochspannungs-Kabeln für Windparkanlagen', *VDE-Hochspannungstechnik*, pp. 750 – 755, Berlin, Germany, 2016.